Characterization of transmitted motion in fetal lung: Quantitative analysis[a)]

Ronald Adler, Jonathan M. Rubin, Peyton Bland, and Paul Carson
Department of Radiology, University of Michigan Medical Center, Ann Arbor, Michigan 48109

(Received 11 April 1988; accepted for publication 21 March 1989)

A simple two-dimensional analytic model is evaluated for transmitted cardiac motion in fetal lung. The model treats the latter as being an incompressible viscoelastic medium. The mean radial deformation in an elastic medium is demonstrated to depend on a length parameter $l \sim \sqrt{\mu/\rho\omega^2}$, where μ, ρ, and ω corespond to elastic shear modulus, mass density, and frequency of cardiac motion, respectively. Digitized M-mode images are demonstrated as a feasible method to measure such deformations *in vivo*. Data for two patients are presented to illustrate the technique.

I. INTRODUCTION

Obstetrical ultrasound provides a useful noninvasive means to both quantitatively and qualitatively assess fetal growth and development. The former usually involves measurement of a length parameter which correlates with mean gestational age and/or fetal well being (i.e., nutritional status).[1] Tissue characterization by prenatal sonography is generally qualitative. A definitive method to quantitate tissue maturity in terms of its dynamical properties, echo texture, etc. is not available at present.[2]

Such characterization would be particularly useful in assessing fetal lung maturity, an important prognosticator of survival of the prematurely born. The existence of such a relationship has been suggested by Birnholz and Farrell,[3] who observed transmitted elastic waves within lung parenchyma by the fetal heart. A "stiff" lung was regarded as being a relatively incompressible medium in which elastic waves are readily propagated to the chest wall. The authors relate their observations to abnormal lecithin/sphingomyelin (L/S) ratios[4] in those prematurely born in their series. Furthermore, soft "compliant", mature fetal lungs were reported not to demonstrate these transmission properties.

Although descriptive evaluation of fetal lung motion may be of value, the relationship between sonographically observed properties and biochemical assessment of fetal lung maturity is not well defined. This is further complicated by inter- and intraobserver variation. However, sonographic changes in fetal lungs most probably occur with maturation, although a quantitative model is not yet available.

Quantitative analysis of fetal lung motion requires the following:

(1) A method whereby small displacements of tissue may be sonographically detected as a function of distance from the epicardial surface.

(2) Identification of the relevant physical parameters determined by such a measurement. For example, local tissue displacements depend both on the inherent bulk properties of tissue as well as the frequency of deformation at the epicardial surface.

Such methods have proven useful in determination of both normal and abnormal patterns of transmitted cardiovascular motion in hepatic parenchyma.[5]

The relationship of these measurements to viscoelastic properties of the medium follows from an appropriate theoretical model of motion dynamics. Within this context, we shall regard the fluid-filled fetal lung as an isotropic incompressible substance subject to relatively small deformations by the adjacent cardiac motion. Fetal lung may then be described in terms of three bulk parameters: density, shear viscosity, and elastic shear modulus. For purposes of illustration, an oversimplified two-dimensional model will be considered herein. Generalization to more complex situations is readily accomplished and will be reserved for a future work.

The feasibility of M-mode scanning to measure local, radially directed displacements will be demonstrated. Digitized M-mode images are utilized to directly measure the radial component of the displacement vector as a function of distance from the pericardial surface, thereby resulting in a measure of transmitted cardiac motion.

II. FETAL LUNG MODEL

For small deformations, the linear theory of viscoelasticity[6] becomes applicable as a description of transmitted elastic waves through fetal lung. Low frequency motion resulting from intermittant respirations are expected to be unimportant for times corresponding to a cardiac cycle. We further neglect pulmonary blood flow as a source of intrinsic transmitted pulsation and small changes in volume that may result from intrabronchial displacement of fluid. Elastic waves resulting from cardiac motion, which occur on time scales $\leqslant 1$ s, are sufficiently low frequency to regard the medium as being incompressible. Thus while local displacements can occur, overall system volume is preserved.

Consider a deformation which takes a vector $\mathbf{r}$ to $\mathbf{r}'$. The corresponding displacement vector

$$\mathbf{u} = \mathbf{r}' - \mathbf{r} \tag{2.1}$$

satisfies

$$\rho \frac{\partial^2}{\partial t^2}\mathbf{u} = \mu\nabla^2\mathbf{u} + \eta\nabla^2 \frac{\partial}{\partial t}\mathbf{u} \tag{2.2}$$

in which ρ, μ, and η refer to mass density, shear modulus, and shear viscosity, respectively. The operations $\partial/\partial t$ and ∇ represent time differentiation and spatial gradient with respect to $\mathbf{r}$. The incompressibility condition requires that

$$\nabla \cdot \mathbf{u} = 0 \,. \tag{2.3}$$

 0094-2405/89/030333-05$01.20

Consider the idealized two-dimensional geometry bounded by the pericardium and chest wall radially, which extends out to infinity in longitudinal dimension (Fig. 1). The latter assumption may be easily extended to finite geometry; however, this simplification is maintained for purposes of illustration. The chest wall is taken as a rigid boundary, which apart from low-frequency respiratory motion, appears to correspond well with qualitative observations using *M*-mode imaging.

The displacement vector **u** then consists of two components

$$\mathbf{u} = \begin{pmatrix} u_x \\ u_y \end{pmatrix}, \tag{2.4}$$

with the boundary conditions

$$u_x(0,y,t) = g(y)\cos(\omega t), \tag{2.5a}$$

$$u_x(a,y,t) = 0, \tag{2.5b}$$

$g(y)$ being the "diastolic" profile. Solution of Eq. (2.2) subject to conditions (2.3) and (2.5) entirely specifies transmitted cardiac motion within the context of this model. The details of this calculation are presented in the Appendix.

It will be convenient to discuss solutions in terms of Fourier transforms.[7] For example, we define

$$\bar{g}(k) = \int_{-\infty}^{\infty} dy\, e^{iky} g(y). \tag{2.6}$$

General solution to Eq. (2.2) subject to conditions (2.3) and (2.5) results in

$$\mathbf{u}(x,y,t) = \frac{1}{2\pi}\,\mathrm{Re}\int_{-\infty}^{\infty} dk\, e^{-i(ky-\omega t)}\bar{g}(k)\,\frac{1}{\sin\xi a} \times \begin{pmatrix} \sin\xi(a-x) \\ -\dfrac{i\xi}{k}\cos\xi(a-x) \end{pmatrix} \tag{2.7}$$

in which ξ is given by Eqs. (A12)–(A15), and Re refers to real component. In a purely elastic medium, $\eta = 0$, Eq. (A12) becomes

$$\xi(k) = \left[\frac{\rho\omega^2}{\mu} - k^2\right]^{1/2}, \tag{2.8}$$

indicating the presence of elastic waves for spatial frequencies

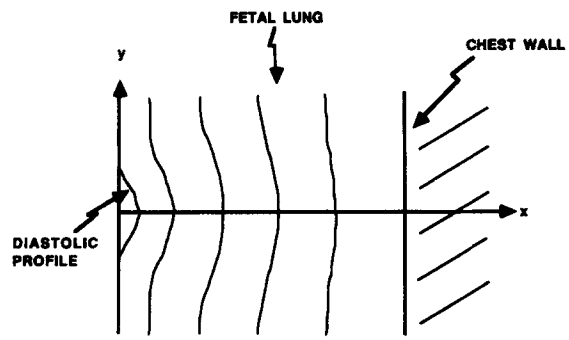

FIG. 1. Schematic of two-dimensional model. Diastolic profile designates the maximal epicardial displacement relative to a fixed base line ($x = 0$). a represents the distance to the chest wall, taken as a rigid boundary. Axial boundaries extend out to infinity.

$$k \leqslant \sqrt{\frac{\rho\omega^2}{\mu}}. \tag{2.9}$$

Higher spatial frequencies result in damping. Alternatively, increasing shear modulus or decreasing heart rate diminishes the maximum spatial frequency at which damping would occur. The effective range of a deformation in an elastic medium is expected to be characterized by a length scale $l \sim \sqrt{\mu/(\rho\omega^2)}$.

Further evaluation of Eq. (2.7) is facilitated by considering a spatially slowly varying surface deformation $g(y)$ such that $\xi(k)$ may be replaced by $\xi(0)$. The radial component $u_x(x,y,t)$ is then approximated by

$$u_x(x,y,t) \simeq \mathrm{Re}\, e^{i\omega t}\,\frac{\sin\xi(a-x)}{\sin\xi a}\,g(y). \tag{2.10}$$

The factor $\sin\xi(a-x)/\sin\xi a$ relates to the maximal deformation profile. Our own experience with fetal *M* mode suggests the maximum deformation occurs at the epicardial surface and declines at the chest wall. For an elastic medium ($\eta = 0$), this would require a physiologic range for ξa:

$$\xi a = \sqrt{\frac{\rho\omega^2 a^2}{\mu}} \in [0,\pi/2]. \tag{2.11}$$

The effectiveness of transmission is readily discussed in terms of the mean radial deformation

$$\langle u_x(x,y,t)\rangle \equiv \frac{1}{a}\int_0^a dx\, u_x(x,y,t) = \frac{1}{2\pi}\,\mathrm{Re}\int_{-\infty}^{\infty} dk\, e^{-i(ky-\omega t)}\hat{g}(k)\frac{1}{\xi a}\tan\frac{\xi a}{2}, \tag{2.12}$$

which is approximated by

$$\frac{\langle u_x(x,y,t)\rangle}{g(y)\cos\omega t} = \sqrt{\frac{\mu}{\rho\omega^2 a^2}}\tan\frac{1}{2}\sqrt{\frac{\rho\omega^2 a^2}{\mu}} \tag{2.13}$$

when $\eta = 0$. In the range $\xi a \in [0,\pi/2]$, Eq. (2.13) takes values between $1/2 \to 2/\pi$. Perceived lung stiffness as defined by Birnholz and Farrell corresponds to larger values of $\langle u_x\rangle$, which occurs for larger values of ω or smaller μ.

These observations do not account for the presence of dissipative forces, which if significant result in diminished range of transmitted pulsations. Inclusion of viscosity results in a complex-valued expression for ξ^2, Eqs. (A12)–(A14). New effective length scales introduced are given by Eq. (A15). For simplicity we consider the low spatial frequency limit (i.e., $k \to 0$). The relative strength of dissipative and elastic forces is determined by the parameter $(\omega\eta/\mu)^2$. Spatial damping due to viscosity will, however, be present, and is determined by $\gamma \sin\theta$ in Eq. (A15). For $(\omega\eta/\mu)^2 < 1$, corresponding to weak viscous contribution, this latter term becomes

$$\gamma\sin\theta \simeq \frac{1}{2}\sqrt{\frac{\rho\omega^2}{\mu}}\left(\frac{\omega\eta}{\mu}\right). \tag{2.14}$$

Therefore, damping appears to increase with increasing heart rate, viscosity, and diminish with increases in shear modulus.

Quantitative evaluation of transmitted cardiac motion in fetal lung would be facilitated by the presence of some global

parameter. A potential candidate is the mean radial displacement, (eg., $\langle u_x \rangle$), as this parameter may be evaluated using *M*-mode analysis by tracking the relative motion of specular reflectors in time. Since such data is inherently noisy, tracking the motion of peaks within the two-time correlation function or alternatively calculation of an appropriate correlation length may be of value. Such investigation is currently in progress. For the simplistic model considered herein, the spatially averaged radial displacement $\langle u_x \rangle$ is given by Eqs. (2.12) and (2.13).

III. METHODS

All images were obtained in sector mode utilizing a 3.5 MHz variable focused phased array scanner (General Electric 3600) with a combined *B* /*M* mode display. Only scans perpendicular to the fetal spine imaging the right ventricle, left ventricle, and interventricular septum were measured (Fig. 2). As noted by Birnholz and Farrell[3] this corresponded to a line of transmitted motion through the right middle lobe and lingula. The resulting *M*-mode images were digitized to a 512×512 matrix using a Vicom 1850 digital image processing system. The film was placed on a light box within the field of view of a video camera adjusted so that the ultrasound image filled the entire digitized image. Since the distances measured in the fetal lungs on the films were relatively short compared to dimensions of the entire frame and since the areas of interest were near the center of the image, the slight degree of spatial distortion in the camera's optics and electronics was deemed acceptable. This assumption is further supported by the fact that relative changes in only immediately adjacent systoles and diastoles were measured.

Radial lines of the data between the epicardium and chest wall corresponding to the maximal epicardial excursion were interactively selected from the digitized images (Fig. 3). Areas in the *M*-mode trace selected for measurement contained well-defined lung motion and had individual reflectors that could be seen extending through a systolic/diastolic couplet. We also required that these reflectors be distributed throughout the fetal lung. The relative displacements of visible reflectors in systolic/diastolic couplets were measured from the digitized image. Verification of reflector locations was facilitated by comparison with plots of the raw data at the corresponding times in the cardiac cycle.

Base line heart/chest wall distance was taken to be the distance from the epicardial reflector to the chest wall in systole. In fact, although the epicardial surface was easy to identify, the precise reflection that represented the chest wall could be difficult to detemine, Fig. 3. However, there was little difficulty narrowing the possibilities down to, at most, two candidate reflections. Since the total epicardial/chest wall thickness is on the order of 2 cm, while the distance between candidate reflections is approximately 1 mm, the linear error is about 5%. We feel that such an error is acceptable in this simplified model.

All length parameters were then normalized relative to this epicardial/chest wall length (denoted as *a*), thereby allowing comparisons of multiple data sets. Empirically, this normalization was chosen to account for slight variations in the epicardial/chest wall distance at different axial planes or due to slight oblique scanning. We further normalized the results of each couplet relative to the maximal displacement as measured by the motion of the epicardial surface. We, therefore, could compare displacements of different amplitudes.

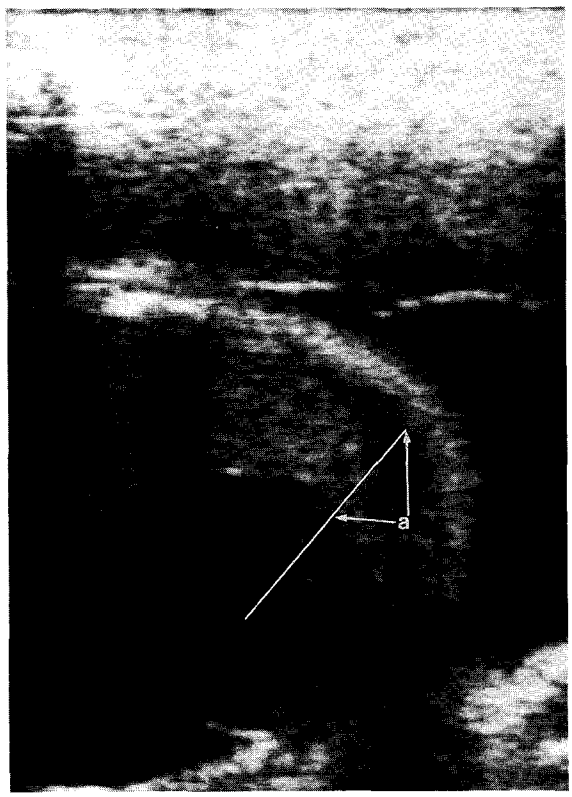

FIG. 2. Two-dimensional sector image obtained through the fetal thorax at the appropriate level for *M*-mode analysis. The *M*-mode line approximates a perpendicular to the interventricular septum. The epicardial/chest wall distance along the *M*-mode line is *a*. The projection of epicardial motion along this line defines *g*.

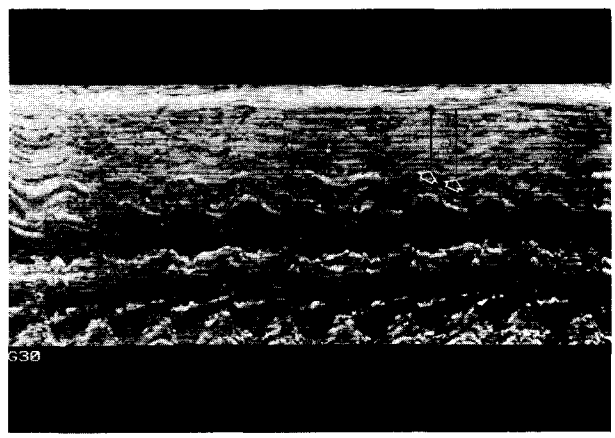

FIG. 3. *M*-mode record from a 30 week fetus demonstrating a typical diastolic/systolic couplet that was digitized to measure relative displacements. The arrows mark the undulating epicardial surface at diastole (left) and systole. The black lines extending radially through the fetal lung to the chest wall from the epicardium denote corresponding lines of data that were compared. The precise positions of reflectors were determined from plots of the raw data.

VI. RESULTS AND DISCUSSION

The anatomic plane of imaging is depicted in Fig. 2. The M-mode line is chosen to approximate a perpendicular to the interventricular septum. A representation M-mode image, Fig. 3, is presented for a 30 week gestation. This demonstrates well defined reflectors, which in many cases persist for multiple cardiac cycles. Identification of these specular reflectors form the basis for the analysis to follow.

Normalized radial displacement per unit epicardial displacement is depicted as a function of distance from the epicardium (Figs. 4 and 5). Normalization with respect to systolic epicardial/chest wall distance a facilitates comparison of different data sets resulting from variation in axial plane or obliquity. Significant transmitted cardiac motion throughout the fetal lung is present in both cases. Absence of radial motion at the chest wall attributable to fetal heart is a consistent finding. The suggested monotonic nature of the radial deformation indicates that the spatial average $\langle u_x \rangle$ should accurately reflect the range or persistence of a propagated surface deformation. Low frequency, somewhat erratic chest wall motion is expected to relate to fetal respiration but as noted above, has little effect on the calculations.

The relatively noisy appearing scatter plots for radial displacement, obtained for individual systolic/diastolic pairs, are expected to relate in part to slight variations in fetal and/or transducer position, as well as measurement error. Further, data normalized for epicardial motion (i.e., dividing u by g) may not be readily superimposed. For the two-dimensional model considered herein, separability only occurs in the Fourier domain, Eq. (A11). In a more complex finite geometry separability may not be readily accomplished. The presence of random scatterers is expected to be a major contributor to fluctuations in the data. Spatial and temporal averaging may be of value in suppressing the latter; this will be the topic of a future work.

While definitive statements regarding fetal lung motion cannot be made on the basis of this limited analysis, transmitted motion would appear to be a feature extending well into pregnancy with possibly increased compressibility with increasing gestational age. Whether this finding is, in fact, correct or is significantly altered in the presence of immaturity is uncertain, and will require further study with a quantifiable parameter (e.g., $\langle u_x \rangle$).

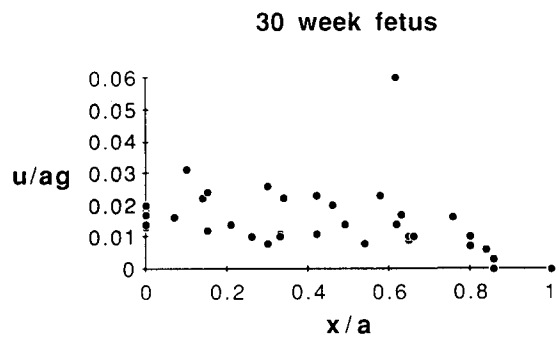

FIG. 4. 30 week gestation. Scatter plot of maximal normalized radial displacement per unit epicardial displacement (u/ag) as a function of normalized distance (x/a) measured from the epicardial echo in systole. Two M-mode records with slightly differing a values were employed with three diastolic/systolic couplets from one record and two from the other.

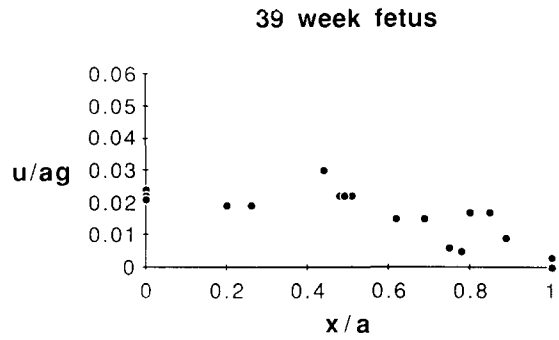

FIG. 5. Scatter plot for 39 week gestation. The axes are the same as in Fig. 3. The data is derived from a single M-mode record with four diastolic/systolic couplets.

In view of the prior analysis, heart rate would appear to be an important factor in the persistence of transmitted motion. Our calculations show that the magnitude of local deformation $\langle u_x \rangle$ motion will vary with heart rate, Eq. (2.13). This is a new and potentially significant result, for it will alter the tissue compressibility measurements in any tissue motion study. Since tissue compressibility is a property being studied both in developing and mature tissues,[3,5] the effect of heart rate will have to be taken into account before results can be compared and analyzed. In this preliminary work, we did not include this effect, since we were only interested in showing trends in our two patients. Future work will account for heart rate by appropriate normalization of any measured displacement parameter.

Clearly, we have made simplifying assumptions in generating this model. First, we assumed that the chest wall is a fixed structure. This assumption appears valid on at least two grounds: (1) the frequency of motion of the chest wall is much lower than that of the epicardial surface, at least by an order of magnitude, and (2) empirically we actually detected very little motion of the chestwall. We have also chosen to ignore the effects of fetal respiration, which might alter the fluid content in the chest. We should note, however, that previous work on this subject has also ignored this possibility.[3] Finally, the assumption of isotropy and the adequacy of radial one-dimensional measurements to detect lung compressibility seem reasonable for this preliminary model.

V. CONCLUSION

A simplified two-dimensional model describing the viscoelastic response of fetal lung to periodic cardiac motion has been presented. In purely elastic media, deformations are characterized by a length scale $l \sim \sqrt{\mu/\rho\omega^2}$ determined by shear bulk modulus μ, frequency ω, and mass density ρ. The parameters μ and ω, therefore, relate reciprocally to the persistence of transmitted motion. A "stiff" lung (i.e., smaller value of μ) should then demonstrate radial displacement closer to the chest wall. Viscosity effects, if important, tend to attenuate elastic waves. Within the context of the model assumptions, a potential physiologic range for ξa is suggested, Eq. (2.11).

M-mode analysis provides a mechanism to quantitate fetal lung motion. Measurement of radial displacement of specular reflectors is accomplished using digital *M*-mode images. Results in two cases demonstrates the feasibility of this technique. A longitudinal study is currently in progress to quantitatively assess whether any clear separation between lung compressibility and gestational age exists. The chest wall appears to act as a rigid boundary to radial lung displacement. In view of imcompressibility, radial motion is compensated by corresponding axial displacement. Digitized two-dimensional sector images may potentially evaluate such motion.

Generalization to more realistic geometries will be of value in assessing the effect of finite axial dimensions of fetal thorax, presence of a diaphragm, etc. Improved data analysis to suppress random noise is expected to make such measurements as described herein accessible to longitudinal studies which evaluate maturity in terms of motion parameters.

APPENDIX

Consider first solution of Eq. (2.2) subject to the boundary condition

$$u_x(0,y,t) = g(y)e^{i\omega t}. \tag{A1}$$

We obtain separable solutions of the form

$$\mathbf{u}(x,y,t) = \mathbf{v}(x,y)e^{i\omega t}, \tag{A2}$$

in which $\mathbf{v}$ satisfies

$$\nabla^2\mathbf{v} + \frac{\rho\omega^2}{\mu + i\omega\eta}\mathbf{v} = 0. \tag{A3}$$

Taking the complex conjugate of Eq. (A3) results in

$$\nabla^2\mathbf{v}^* + \frac{\rho\omega^2}{\mu - i\omega\eta}\mathbf{v}^* = 0. \tag{A4}$$

so that $\mathbf{v}^*$ is a solution of Eq. (2.2) subject to the boundary condition

$$u_x(0,y,t) = g(y)e^{-i\omega t}, \tag{A5}$$

therefore,

$$\mathbf{u}(x,y,t) = \mathrm{Re}\,\mathbf{v}(x,y)e^{-\omega t}, \tag{A6}$$

is a solution of Eq. (2.2) which satisfies Eq. (2.5a), and Re refers to real component. In terms of the new vector $\mathbf{v}$, the incompressibility condition becomes

$$\nabla\cdot\mathbf{v} = 0, \tag{A7}$$

or utilizing the Fourier transform of $\mathbf{v}$,

$$\bar{\mathbf{v}}(x,k) \equiv \int_{-\infty}^{\infty} dy\, e^{iky}\mathbf{v}(x,y) \tag{A8}$$

enables evaluation of $\bar{v}_y$ in terms of $\bar{v}_x$:

$$\bar{v}_y(x,k) = \frac{i}{k}\frac{\partial}{\partial x}\bar{v}_x(x,k). \tag{A9}$$

We need only solve Eq. (A3) for $\bar{v}_x$ subject to appropriate boundary conditions:

$$\left[\frac{\partial^2}{\partial x^2} + \left(\frac{\rho\omega^2}{\mu + i\omega\eta} - k^2\right)\right]\bar{v}_x = 0, \tag{A10}$$

resulting in

$$\bar{v}_x = \bar{g}(k)\frac{\sin\xi(a-x)}{\sin\xi a}, \tag{A11a}$$

$$\bar{v}_y = -i\frac{\xi}{k}\bar{g}(k)\frac{\cos\xi(a-x)}{\sin\xi a}, \tag{A11b}$$

where

$$\xi^2 \equiv \frac{\rho\omega^2}{\mu + i\omega\eta} - k^2. \tag{A12}$$

It will be convenient to reexpress ξ^2 in terms of its modulus and phase. We therefore define

$$\xi^2 = \gamma^2 e^{2i\theta}, \tag{A13}$$

where

$$\gamma^2 = \frac{\{[\rho\omega^2\mu - k^2(\mu^2 + \omega^2\epsilon^2)]^2 + (\rho\omega^3\eta)^2\}^{1/2}}{[\mu^2 + \omega^2\eta^2]}, \tag{A14a}$$

$$\tan 2\theta = \frac{\rho\omega^3\eta}{\{[\rho\omega^2\mu - k^2(\mu^2 + \omega^2\eta^2)]^2 + (\rho\omega^3\eta)^2\}^{1/2}}. \tag{A14b}$$

In particular, evaluation of the length parameters $\gamma\cos\theta$ and $\gamma\sin\theta$ will be useful:

$$\gamma\cos\theta = \frac{1}{\sqrt{2}}\left\{\gamma^2 + \frac{[\rho\omega^2\mu - k^2(\mu^2 + \omega^2\eta^2)]}{\mu^2 + \omega^2\eta^2}\right\}^{1/2}, \tag{A15a}$$

$$\gamma\sin\theta = \frac{1}{\sqrt{2}}\left\{\gamma^2 - \frac{[\rho\omega^2\mu - k^2(\mu^2 + \omega^2\eta^2)]}{\mu^2 + \omega^2\eta^2}\right\}^{1/2}. \tag{A15b}$$

[a] This work was supported in part by PHS Grant No. R01HD17243 awarded by the National Institute for Human Growth and Development (DDHS).

[1] P. W. Callen, *Ultrasonography in Obstetrics and Gynecology* (Saunders, Philadelphia, 1983).

[2] P. L. Carson, C. R. Meyer, R. A. Bowerman, P. H. Bland, and F. L. Bookstein, "Prediction of Pulmonary Maturity From Ultrasound Scattering," *Tissue Characterization with Ultrasound,* edited by J. F. Greenleaf (Chemical Rubber, Boca Raton, FL 1986), pp. 169–187.

[3] J. C. Birnholz and E. E. Farrell, "Fetal Lung Development: Compressibility as a Measure of Maturity," Radiology **157**, 495–498 (1985).

[4] J. R. Wilson and E. R. Carrington, *Obstetrics and Gynecology,* 6th ed. (Mosby, St. Louis, Missouri, 1979).

[5] M. Tristam, D. C. Barbosa, D. O. Cosgrove, D. K. Nassiri, J. C. Bamber, and C. R. Hill, "Ultrasound Study of in Vivo Kinetic Characteristics of Human Tissues," Ultrasound Med. Biol. **12**, 927–937 (1986).

[6] L. D. Landau and E. M. Lifshitz, *Theory of Elasticity,* 2nd ed. (Pergamon, New York, 1970).

[7] R. Dennery, and X. Krzywicki, *Mathematics for Physicists* (Harper and Row, New York, 1967).